Imaging and Discrimination of High-Z Materials with Muon Scattering Tomography

L. Frazão,[1,*] S. Maddrell-Mander,[1] C. Thomay,[1] J. Velthuis,[1] and C. Steer[2]

[1] *University of Bristol*
[2] *AWE*

We have developed methods to define the edges of uranium blocks embedded in concrete, and to discriminate them from different high-Z materials, using Muon Sattering Tomography. Nuclear waste can be stored in concrete containers, whose disposal is an important matter. Legacy nuclear waste includes containers with unknown materials. It is important to develop methods to scan nuclear waste vessels without opening them. Muon Scattering Tomography is a non-invasive technique that can be used for this purpose, using as probes the natural occurring cosmic muons, which are highly penetrating particles. We carried out simulations in Geant4 of uranium objects of different lengths, enclosed in concrete. These lengths were measured with a new algorithm and compared to the simulated lengths, resulting in a resolution of 0.9 mm, with a 0.2 mm error. The smallest length measured was a uranium sheet with a width of 2 mm. For the material discrimination study, a multivariate analysis was performed in order to distinguish materials from different simulations with the same geometry. Cubic blocks of different sizes and materials were simulated, with sides ranging from 2 cm to 10 cm, and scanning times ranging from a few hours up to 80 hours depending on the sizes of the blocks. We show that it is possible to distinguish uranium blocks from lead, tungsten and plutonium blocks of the same size. The smallest blocks with a good discrimination were cubes with 2 cm side (and 3 cm for discrimination between uranium and plutonium).

I. INTRODUCTION

The management and disposal of nuclear waste requires the knowledge of the materials present in the containers. There is therefore a need to characterise concrete containers of nuclear waste without having to open them. This is particularly important for legacy waste, which includes large containers with unknown materials, which might have undergone changes over time.

Muon scattering tomography (MST) is a technique that uses cosmic muons to scan large vessels [1]. Muons are high energy particles formed in the Earth's atmosphere as a product of the collision of primary cosmic rays with the air atoms. The muon flux at ground level is about 1 muon per cm^2 per minute. MST allows for the Knowing the position and shape of materials is useful for hazard assessment.

Muons undergo multiple scattering in matter [2, 3], where the distribution of the projected scattering angles is approximately Gaussian, whose standard deviation σ depends on the radiation length of the material traversed as

$$\sigma \approx \frac{13.6 \text{ MeV}}{\beta c p} z \sqrt{X/X_0}(1 + 0.038 \ln(X/X_0)), \qquad (1)$$

where p is the momentum of the muon, βc its velocity, z its charge number, X the thickness of the material, and X_0 the radiation length [4] which is given by

$$X_0 \approx \frac{A \cdot 716.4 \text{ g/cm}^2}{\rho \cdot Z(Z+1) \ln(287/\sqrt{Z})}, \qquad (2)$$

where A is the mass number, Z the atomic number and ρ the density.

* leonor.frazao@bristol.ac.uk

II. METHODS

Figure 1 illustrated the principle of MST. The muons are tracked before and after crossing the volume to be scanned, and a fit is performed over the muon hits in the detectors. The angle can then be measured.

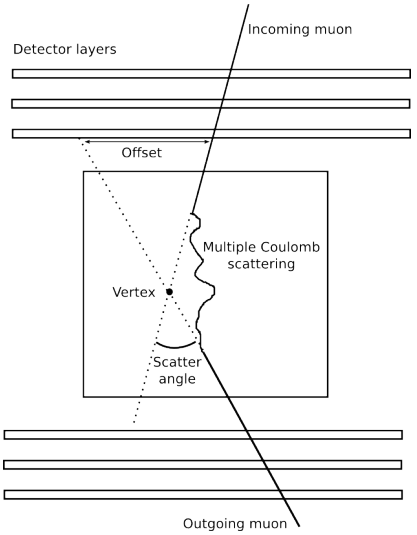

FIG. 1: Illustration of the muon scattering principle and some variables obtained.

Simulations were performed in Geant4, which is a toolkit that simulated the passage of particles through matter [5]. The muon source used was CRY [6], which creates cosmic muon energy and angle spectra from real data.

The detectors simulated had a 1×1 m^2 active area and a 450 μm intrinsic resolution, taken from the value of real RPCs (resistive plate chambers), measured and published in [7]. Three pairs of RPCs were place above and below the volume of interest. Each pair had a detector for the X and another for the Y direction, like the

ones used in the RPC experiments.

The concrete drum simulated was a cylinder with 40 cm of length and 13 cm of radius. The objects to be measured inside were blocks of high-Z materials of different sizes.

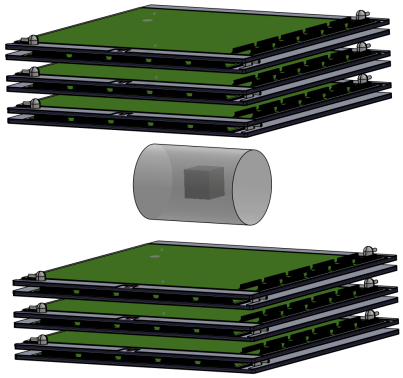

FIG. 2: Illustration of the simulation geometry.

III. IMAGING

An algorithm to find high-Z materials was developed in [8] and applied to imaging of nuclear waste in [9], where it is shown that lumps of high-Z materials can be found inside concrete. A first edge finding algorithm was also shown. In this paper, a new edge finding algorithm will be described.

A. Imaging algorithm

The method described in [8] and in [9] divides the volume in cubic bins of 1 cm^3. A weighted metric distance is calculated for each pair of vertices reconstructed in a bin as

$$m_{ij} = \frac{\|v_i - v_j\|}{(\theta_i p_i)(\theta_j p_j)}, \tag{3}$$

where v_i is the reconstructed vertex position of muon i, θ_i its scatter angle and p_i its momentum. This is done for a fixed number of the 26 most scattered vertices in each bin, which results in 325 entries of m_{ij}. The bins were shifted by 1 mm nine times in order to improve the imaging resolution.

The distributions of m_{ij} for each bin were fitted with Landau distribution convoluted with a Gaussian. Several variables from the distributions and the fitted functions were used in a multivariate analysis (MVA), such as the widths, the peak amplitude and position, the maximum value and respective bin position. The MVA method used was the Fisher linear discriminant [10], which outputs a probability value between 0 and 1 of a bin being in concrete or uranium. This method was trained with data from a pure concrete and a pure uranium sample, which resulted in the probability values shown in Figure 3.

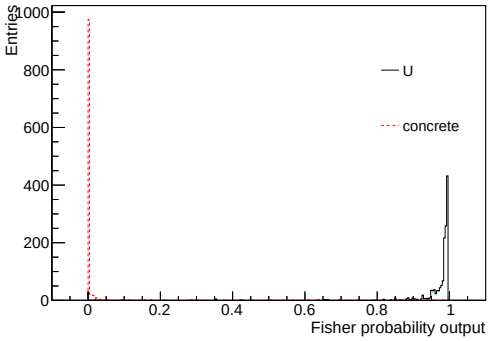

FIG. 3: Output from the training with the Fisher linear discriminant, using samples of pure concrete and pure uranium.

B. Results

Blocks of uranium of different sizes were simulated, with lengths in the X direction (the one to be measured with the previous algorithm) ranging from 0.2 cm to 10 cm. The blocks with lengths over 3 cm were cubic, while the smaller ones always had 3 cm in Y and Z. A value of the Fisher probability was obtained for each bin shift of 1 mm. Examples of these values are shown in Figure 4, where the uranium blocks can clearly be distinguished from the concrete background.

The lengths of these blocks were measured and compared to the real simulated lengths. A linear relation was observed. A linear function was fitted and used to calibrate the measured lengths, which can be seen in Figure 5. The smallest lengths measured are depicted in Figure 6.

From the data in Figure 5 a resolution σ was calculated as

$$\sigma = \sqrt{\frac{\sum_i (l_t - l_{r,i})^2}{n}}, \tag{4}$$

where l_t is the true simulated size, $l_{r,i}$ the reconstructed sizes, and n the number of data points used. A good resolution was obtained, of $\sigma = 0.9 \pm 0.2$ mm.

IV. MATERIAL DISCRIMINATION

It is important not only to find high-Z materials in nuclear waste, but also to be able to identify which materials they are. A method to discriminate between uranium and other high-Z materials (lead, tungsten and plutonium) was developed, as described in this section [11].

A. Methods

Several variables from the MST simulation were used in an MVA using the Fisher linear discriminant. These variables were the 2D projected and 3D scatter angles, the offsets between the measured and the extrapolated hit positions, the χ^2 of a linear fit over all the hits in the upper and lower detectors, the χ^2 of the combined fit of

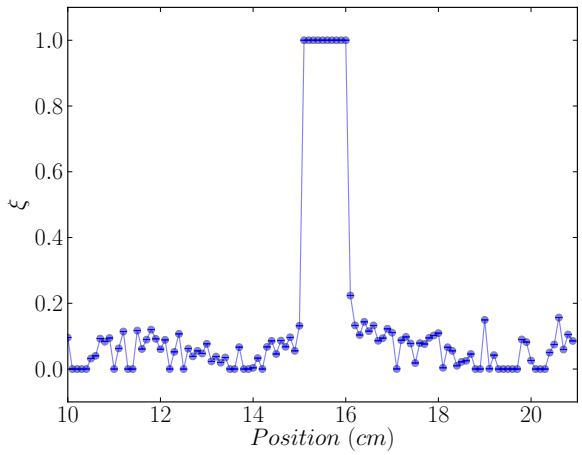

(a) 0.5 cm

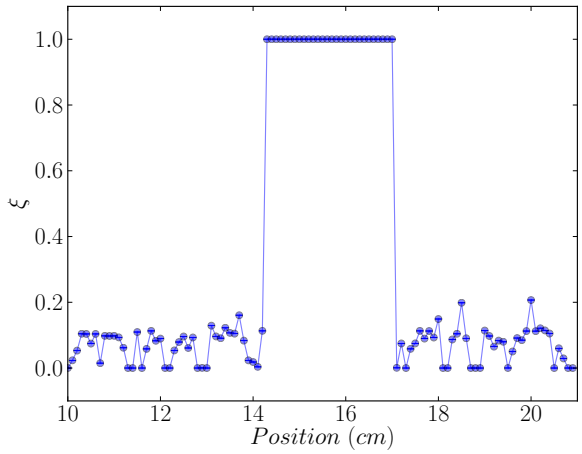

(b) 3 cm

FIG. 4: Fisher probability output, ξ, as a function of the x coordinate for a 0.5 cm (a) and a 3 cm block (b) of uranium inside concrete.

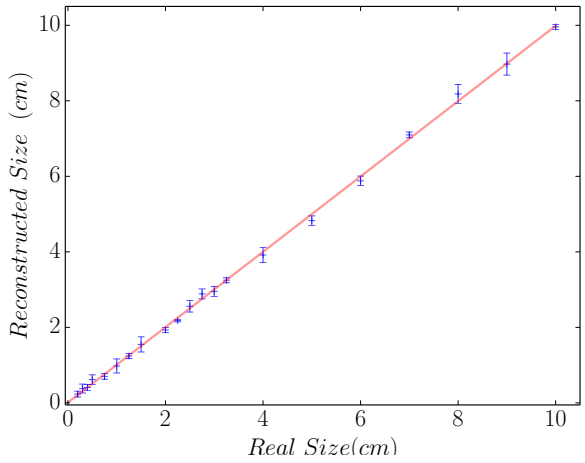

FIG. 5: Reconstructed length against real length.

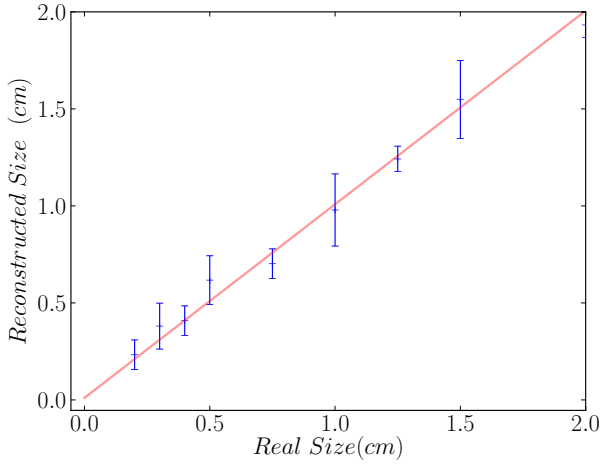

FIG. 6: Reconstructed length against real length for the smallest lengths.

incoming and outgoing tracks and reconstructed vertex, and the momentum of the muon. The MVA was trained with data from a block of uranium and a block of each of the other materials. An example of the output obtained for the training comparing uranium to lead can be seen in Figure 7. Although they overlap, the distributions are different, Therefore, several of these distributions were obtained, and their mean was used as a discriminator value to distinguish both materials.

An example of the values obtained for the mean for uranium and lead is shown in Figure 8a. In order to assess the performance of the material discrimination, ROC graphs (Receiver Operating Characteristics) were obtained from the distributions of the means. These graphs compare the true positive rate (in this case, when uranium is correctly classified) versus the false positive rate (when another material is wrongly classified as uranium). An example of a ROC graph can be seen in Figure 8b. A measure of how well the materials are separated is the area under the curve (AUC) of the ROC graphs. An AUC of 50% is a random classifier, while an ideal classifier would have an AUC of 100%.

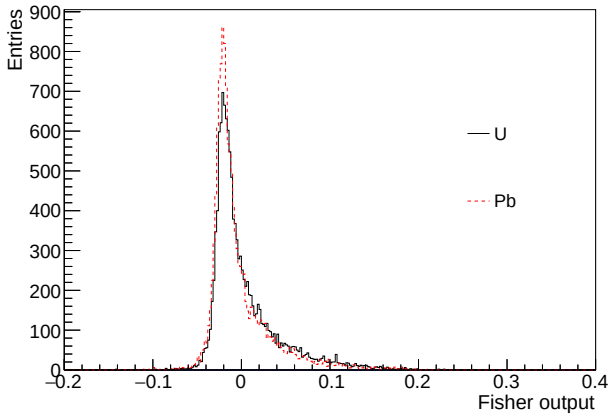

FIG. 7: Output of the Fisher MVA method, comparing uranium and lead, for a $10 \times 10 \times 10$ cm^3 block.

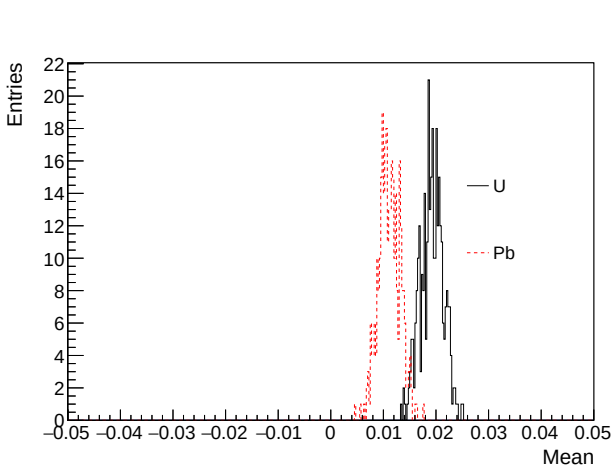

(a)

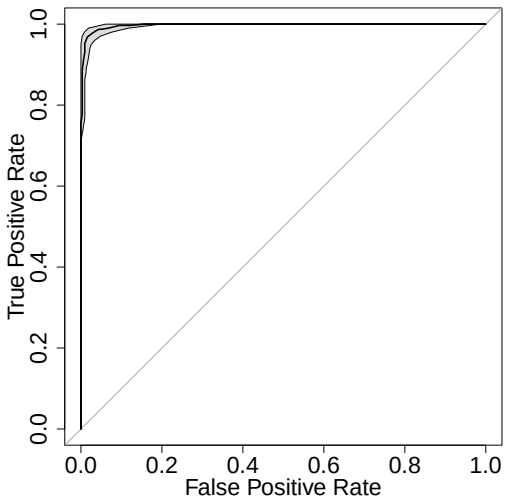

(b)

FIG. 8: Mean value (a) and ROC curve (b) from the Fisher discriminant method, distinguishing Uranium from Lead, $10 \times 10 \times 10$ cm^3 cube, 1h.

B. Results

The simulation and material discrimination analysis were performed over several cube block of different sizes, with sides of 1 cm, 2 cm, 3 cm, 5 cm and 10 cm. The AUC obtained from comparing uranium to lead and tungsten can be seen in Figures 9 and 10, for shorter and longer periods of data taking time respectively. It can be seen that for larger blocks, material separation can be done after a short period of time, while for larger ones more data is needed, up to about 70h for a $2 \times 2 \times 2$ cm^3 block. It was not possible to distinguish the $1 \times 1 \times 1$ cm^3 blocks, as Figure 10 shows the AUC not much above 50%.

The results obtained for the comparison between uranium and plutonium are shown in Figure 11. In this case, the smallest block measured was $3 \times 3 \times 3$ cm^3, as smaller volumes could not be distinguished. Additionally, a longer muon exposure time was needed, of 200h, and the maximum AUC obtained was 80%. There is some discrimination between these materials, although not a perfect one.

V. CONCLUSIONS

Muon scattering tomography is a useful technique, in particular when applied to scanning nuclear waste.

We have shown an imaging method that can find lumps of high-Z materials in concrete, and which can also be applied to identify the edges of uranium blocks with a very good resolution of $\sigma = 0.9 \pm 0.2$ mm. The smallest length measured was 0.2 cm.

In addition, a method to distinguish between different high-Z materials was developed. This is very important because the requirements for the disposal of nuclear waste depends on the materials it contains. We have shown that it is possible to distinguish uranium from tungsten and lead, for blocks of $2 \times 2 \times 2$ cm^3 or bigger. We have also shown some discrimination power between uranium and plutonium, for blocks of at least $3 \times 3 \times 3$ cm^3.

[1] K. N. Borozdin et al. Surveillance: Radiographic imaging with cosmic-ray muons. *Nature*, 422(March):277, 2003.

[2] V. L. Highland. Some practical remarks on multiple scattering. *Nuclear Instruments and Methods*, 129(2):497–499, 1975.

[3] G. R. Lynch and O. I. Dahl. Approximations to multiple Coulomb scattering. *Nuclear Instruments and Methods in Physics Research Section B: Beam Interactions with Materials and Atoms*, 58(1):6–10, 1991.

[4] K. A. Olive and Others. Review of Particle Physics. *Chin. Phys. C*, 38(9), 2014.

[5] S. Agostinelli et al. GEANT4—a simulation toolkit. *Nuclear instruments and methods in physics research section A: Accelerators, Spectrometers, Detectors and Associated Equipment*, 506(3):250–303, 2003.

[6] C. Hagmann et al. Cosmic-ray shower generator (CRY) for Monte Carlo transport codes. In *Nuclear Science Symposium Conference Record, 2007. NSS'07. IEEE*, volume 2, pages 1143–1146. IEEE, 2007.

[7] P. Baesso et al. A high resolution resistive plate chamber tracking system developed for cosmic ray muon tomography. *Journal of Instrumentation*, 8(08):P08006, 2013.

[8] C. Thomay et al. A binned clustering algorithm to detect high-Z material using cosmic muons. *Journal of Instrumentation*, 8(10):P10013, 2013.

[9] C. Thomay et al. Passive 3D imaging of nuclear waste containers with Muon Scattering Tomography. *Journal of Instrumentation*, 11(03):P03008, 2016.

[10] R. A. Fisher. The use of multiple measurements in taxonomic problems. *Annals of eugenics*, 7(2):179–188, 1936.

[11] Frazão L. et al. Discrimination of high-Z materials in concrete-filled containers using muon scattering tomogra-

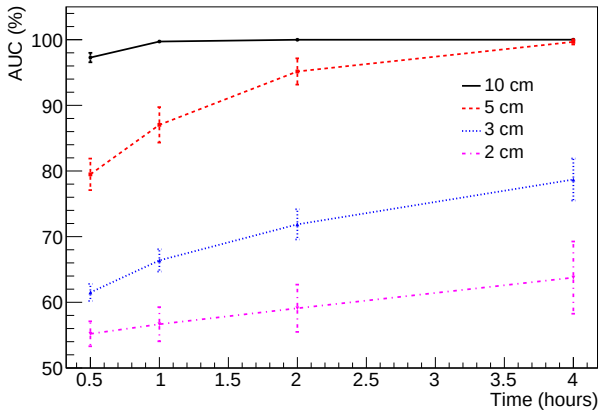

(a) Uranium vs Lead

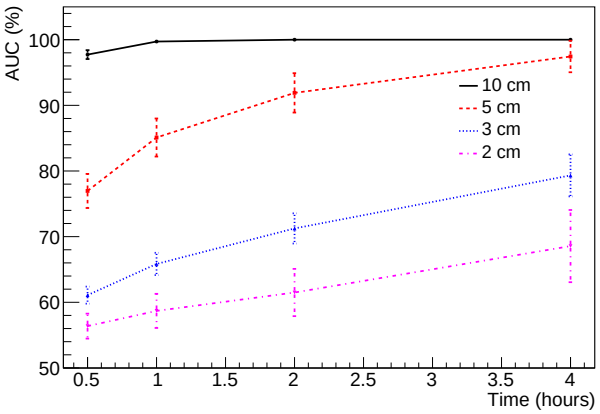

(b) Uranium vs Tungsten

FIG. 9: Area under the curve of ROC curves distinguishing Uranium from Lead (a) and Uranium from Tungsten (b), for different block sizes. The error bars are the confidence intervals of the AUC.

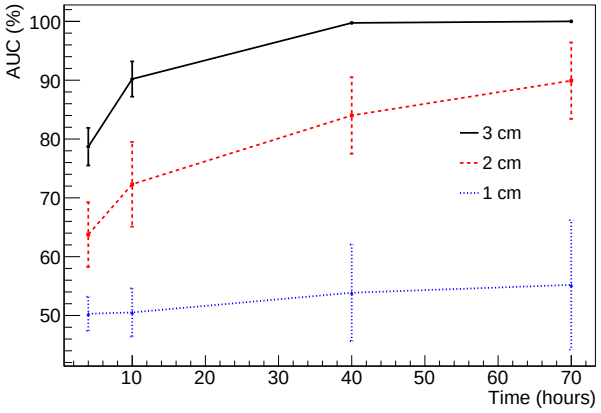

(a) Uranium vs Lead

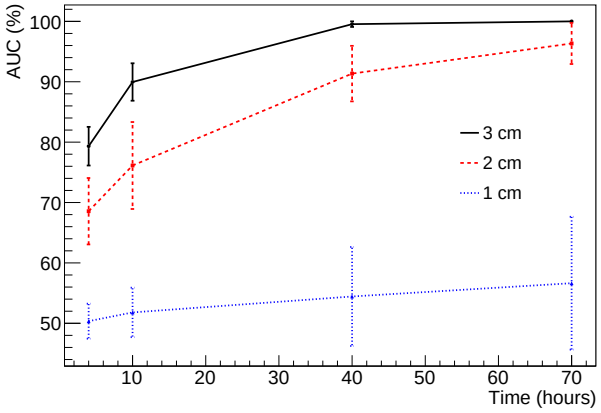

(b) Uranium vs Tungsten

FIG. 10: Area under the curve of ROC curves distinguishing Uranium from Lead (a) and Uranium with Tungsten (b), for different block sizes.

phy. *Journal of Instrumentation*, 11(07):P07020–P07020, 2016.

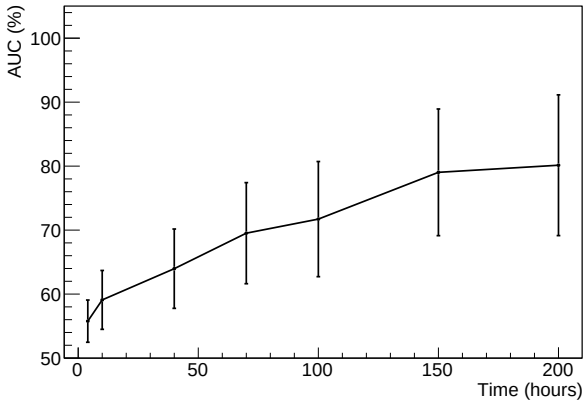

FIG. 11: Area under the curve of ROC curves distinguishing uranium from plutonium for a $3 \times 3 \times 3$ cm^3 block.